Available online at www.sciencedirect.com
SCIENCE DIRECT®
Journal of Power Sources 133 (2004) 79–86
JOURNAL OF POWER SOURCES
www.elsevier.com/locate/jpowsour

Thermal runaway in valve-regulated lead-acid cells and the effect of separator structure

B. Culpin*

11, Bluebell Close, Whittle-le-Woods, Chorley PR6 7RH, UK

Received 23 July 2003; accepted 30 September 2003

Abstract

Thermal runaway is normally defined as the increase in charge or float current that occurs as a result of the increase in cell temperature from the initial applied constant potential. If left unchecked, the currents can reach high values and, ultimately, lead to the destruction of the cell. This definition does not explain why all cells floated at constant potential do not suffer from thermal runaway. The aim of this paper was to investigate and explain the cause of this transition from normal stable behaviour to unstable thermal runaway.

A series of 6 V, 100 A h, valve-regulated lead-acid (VRLA) batteries were overcharged at potentials of up to 2.65 V per cell and the currents, temperatures and gas-evolution rates measured during thermal runaway. From these results, it was concluded that separator dry-out was the critical parameter that controls thermal runaway behaviour. This conclusion was reinforced by other data for the effect of saturation on the resistance, the normal float behaviour and the gas transport in VRLA separators.

A model of the structure of partially saturated separators was developed to explain the observed behaviour, and was used to predict possible improvements in separator structure to increase resistance to runaway.
© 2003 Elsevier B.V. All rights reserved.

Keywords: Battery; Lead-acid; Saturation; Separator dry-out; Thermal runaway; Valve-regulated

1. Introduction

The problem of thermal runaway in sealed nickel–cadmium cells is well known and chargers either use constant current or some form of modified constant potential to avoid the problem. There is no such widespread problem in valve-regulated lead-acid (VRLA) cells. Nevertheless, thermal runaway has been recognised as a possible failure mode in VRLA cells [1] although its incidence is small [2–4]. There is little experimental evidence in the open literature to assist the understanding of the important parameters that result in runaway. It is generally believed, however, that float potential, separator dry-out, temperature and insulation are of importance [5–7].

Thermal runaway is usually considered to be the result of positive feedback of current and temperature when a cell is placed on float charge at constant potential. The initial float current flowing through the cell causes an increase in cell temperature, this causes an increase in current that further increases the temperature until both current and temperature reach high values. Berndt [5] suggests that the phenomenon arises because heat generation has an exponential relationship with temperature but heat dissipation has a linear relationship. This explanation does not indicate why cells under normal float conditions do not experience runaway. There must be some parameter, or set of parameters, that changes normal well-behaved float behaviour into runaway. The purpose of this paper is to establish the required conditions. Published studies that describe incidences of thermal runaway do not take the experiments to completion [7], although reports of fires and even explosions resulting from runaway occur in the literature [3,4]. In the investigations reported here, thermal runaway experiments are taken to completion in order to evaluate the full effects of a runaway event. A theory is developed to explain the essential details of thermal runaway in VRLA cells and ways in which cells can be designed to minimise the problem are postulated.

2. Experimental

All experiments were carried out with single VRLA batteries (6 V, 100 A h) that were designed for standby applications. Most trials were conducted on new batteries but, for

* Tel.: +44-1257-270439.
E-mail address: bculpin@beeb.net (B. Culpin).

0378-7753/$ – see front matter © 2003 Elsevier B.V. All rights reserved.
doi:10.1016/j.jpowsour.2003.09.078

Table 1
Experimental conditions and measurements taken

Cell age	Potential (V)	Test temperature (°C)	Battery temperature measured	Gas collection
New	2.40	20	No	No
New	2.40	40	No	No
New	2.40	60	No	No
New	2.62	40	No	No
New	2.65	20	Yes	Yes
New	2.65	60	Yes	Yes
Old	2.40	20	Yes	Yes
Old	2.40	20	Yes	Yes
Old	2.65	60	Yes	No

comparison, some old batteries that had seen 10 years service and gave 80% rated capacity (i.e., at end-of-life) were also used. For each test, the battery was placed on float at 2.28 V per cell (Vpc) and at the required test temperature until the float current was stable. This was normally 24 h. The float potential was then raised to the test potential and the current allowed to rise without any limit. During the experiment, the current was monitored at regular intervals. In some tests, the case temperature was monitored with a thermocouple and the evolved gas measured by collection over water. The composition of the evolved gas was determined by gas chromatography. A full list of the tests is given in Table 1.

3. Results

3.1. Current profiles

The current profiles for new batteries during the first 100 days of the trial are given in Fig. 1. The data reveal several important characteristics. The currents generally show a slow increase for a period, followed by a rapid rise to thermal runaway. Peak currents are of the order of 50 A. This is followed by an even more rapid decrease to virtually zero current. Applied potential was the main driver for thermal runaway; all batteries at 2.62–2.65 Vpc exhibited thermal runaway, whereas those at 2.40 Vpc showed a much lower and more uncertain trend to runaway. In fact, at this lower voltage, it was taking in excess of 50 days for the current to reach high levels and it is debatable if this can be termed thermal runaway. It is interesting that temperature is shown here not to be a cause of runaway. It does, however, act as an accelerating factor, i.e., all the batteries at 2.65 Vpc suffered runaway, but those at the higher ambient temperature were the first to display the effect. The final point of interest worth noting is the length of time it took to achieve runaway. Even under the most severe conditions of 2.65 Vpc and 60 °C, almost a day elapsed before runaway occurred. At a potential of 2.40 Vpc, the time involved becomes very long indeed. Data for the full test period of 340 days are presented in Fig. 2. Even at this stage, the 2.4 Vpc/40 °C battery displayed no sign of runaway. It is therefore concluded that the critical factor for thermal runaway is a charge/float potential in excess of 2.4 Vpc.

3.2. Temperature profiles

The temperature profiles for two new batteries run at 2.65 Vpc are shown in Fig. 3. As would be expected, the battery temperature followed the same profile as the current. The temperature peaked at 80–90 °C. As this was measured on the exterior of the battery case, the internal cell temperature would be somewhat higher. At the peak of the runaway event, steam was emitted from the vent, which indicated that the electrolyte was near boiling point. Other than the emission of steam and some distortion of the case, no other deleterious effect was found. Liquid was not ejected and the integrity of the case was not effected. Examination of the batteries at the end of the experiment showed that, apart from drying-out of the cells, no other defects in the cell elements had resulted.

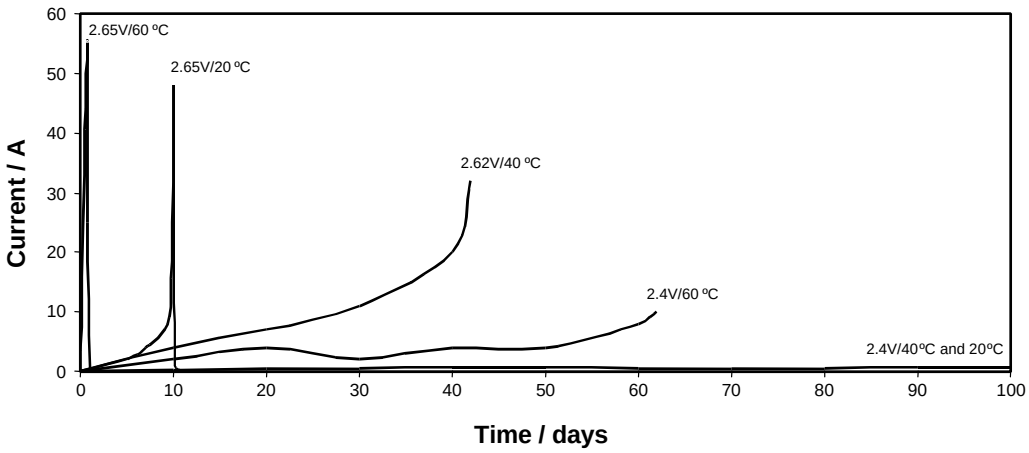

Fig. 1. Current profiles for new batteries for first 100 days.

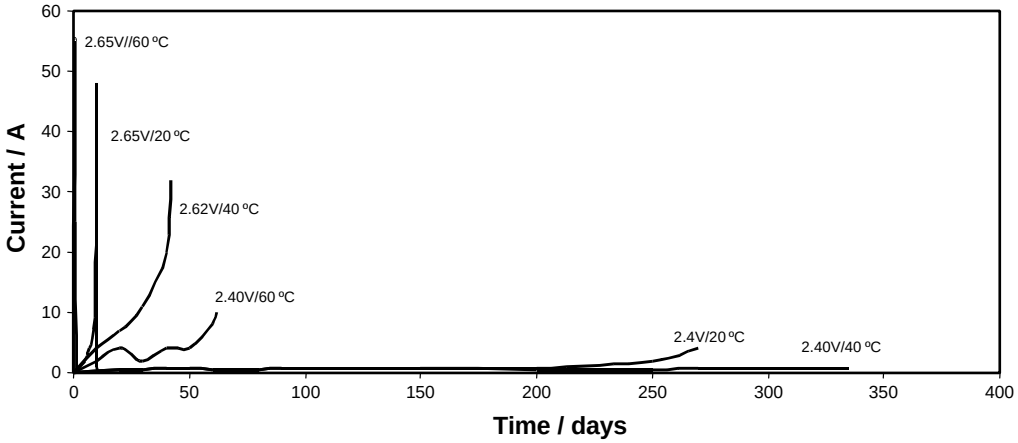

Fig. 2. Current profiles for new batteries for full 340-day trial.

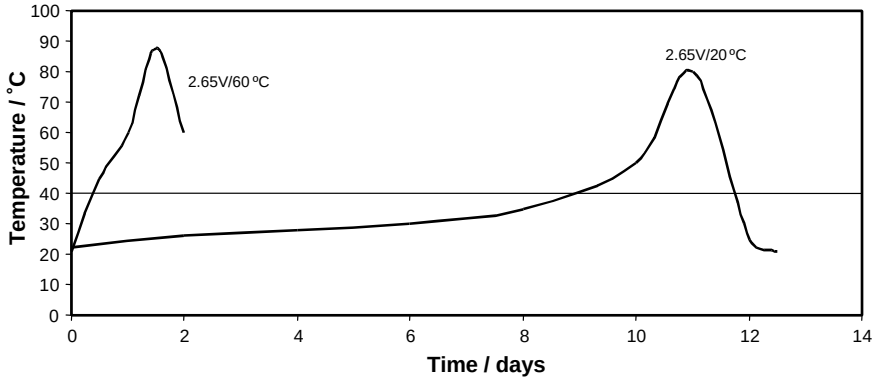

Fig. 3. Temperature profiles for new batteries.

3.3. Thermal runaway in old batteries

The current profile of an old battery at an applied potential of 2.65 Vpc and 60 °C is shown in Fig. 4. In comparison with a new battery under equivalent conditions, the behaviour is much milder and the current only reaches 12 A. The dramatic fall in current after the peak current is absent for the old battery. The temperature (Fig. 4) again follows the same profile as the current, but has a correspondingly lower value because of the lower current. The maximum temperature recorded is 73 °C.

At the lower potential of 2.4 Vpc and 20 °C, no thermal runaway occurred even after 450 days on test. A new battery ran in comparison at the same time gave similar currents, as shown in Fig. 5.

The above observations are of some importance, as anecdotal evidence suggests that old batteries are more likely to give thermal runaway than new ones. The data collected

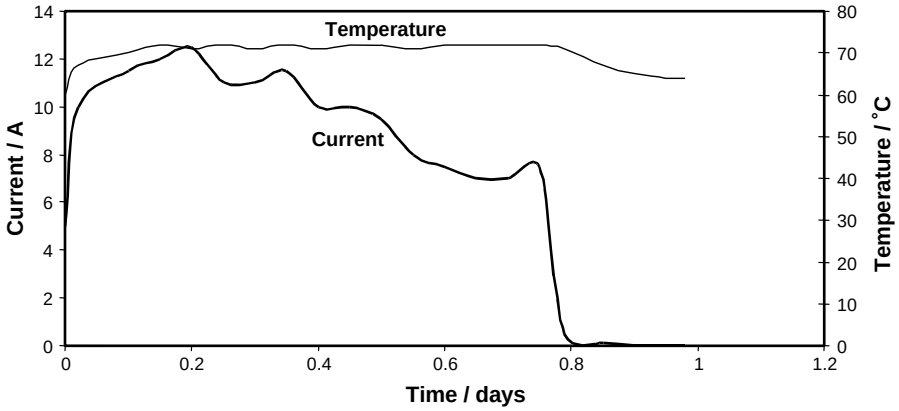

Fig. 4. Current and temperature profile for old batteries at 2.65 Vpc and 60 °C.

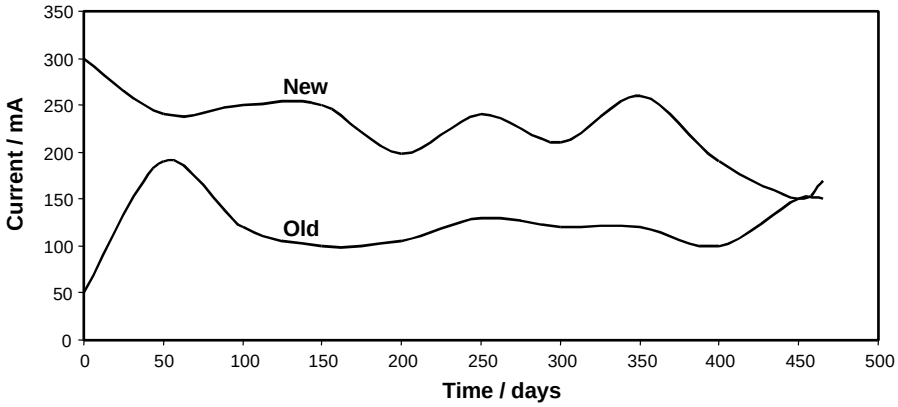

Fig. 5. Comparison of currents for new and old batteries at 2.40 Vpc and 20 °C.

here have shown this to be not true. In fact, although old batteries experience runaway under the same conditions as new batteries, the severity of the event is much less. This is probably due to the old batteries having a higher internal resistance than new ones, as a result of grid corrosion and some loss of water during service from normal recombination inefficiencies.

3.4. Gas evolution

The hydrogen evolution measurements listed in Table 2, together with other available data and recombination efficiencies, show that the VRLA system is able to recombine oxygen at potentials as high as 2.40 Vpc. When the applied potential reaches 2.65 Vpc, however, the recombination efficiency (RE) is virtually zero. This potential dependency on recombination and water loss is important in understanding the mechanism of thermal runaway.

It is important to note the differences between oxygen recombination efficiency and oxygen recombination current. In the context of this paper, the oxygen recombination efficiency is defined as the oxygen recombined compared with the total oxygen that would be generated by the appropriate overcharge current without recombination. It is normally expressed as a percentage and determined by measuring the evolved hydrogen or oxygen. (Oxygen recombination inefficiency results in an equivalent amount of hydrogen being evolved at the negative.) Recombination current is defined as the amount of oxygen transported through the separator and recombining at the negative electrode; it is measured in mA or A. Thus, it is possible to have a high recombination efficiency but a low recombination current.

Table 2
Hydrogen evolution rates

Cell age	Potential (V)	Ambient (°C)	Current gas measured at (A)	Hydrogen evolution rate/cell	RE[a] (%)
New	2.65	20	10	4.2 $dm^3 h^{-1}$	7
New	2.65	60	10	4.1 $dm^3 h^{-1}$	8
New	2.35	40	0.4	0.008 $dm^3 h^{-1}$	95
New	2.27	49	0.3	0.007 $dm^3 h^{-1}$	95
New	2.27	71	0.4	0.017 $dm^3 h^{-1}$	90
New	2.4	20	0.2	0.007 dm^3 per day	98
Old	2.4	20	0.15	0.017 dm^3 per day	97

[a] Recombination efficiency.

3.5. Battery integrity

In all the experiments, the batteries failed in a safe state. The cases although distorted remained leak proof, no explosion or fire occurred, and no acid was ejected from the vents. At the more extreme conditions, the hydrogen evolution rates were high and given an external source of ignition a fire or explosion could have occurred.

4. Discussion

4.1. Mechanism of thermal runaway

The current–time profiles shown in Figs. 1 and 2 show three distinct regions, an initial slow increase in current followed by a rapid rise into runaway and a final more rapid decrease to zero. A mechanism of runaway needs to explain these three separate regions.

The main controlling factor that governs thermal runaway is the applied potential. At values over 2.4 Vpc, runaway will eventually occur, below 2.4 Vpc it does not happen. As shown in Table 2, recombination is very low at potentials above 2.4 V. Thus, it is apparent that water loss is the underlying cause that sends a system into runaway. Further analysis of the curves shown in Figs. 1 and 2 support this. The initial semi-stable period on these curves, where the current is increasing slowly, before the main thermal runaway event, all show a similar number of A h, i.e., a specific A h overcharge has to be passed through the system before true runaway occurs and this value is independent of temperature or potential. Obviously, at higher ambient temperatures and applied potentials, the initial current will

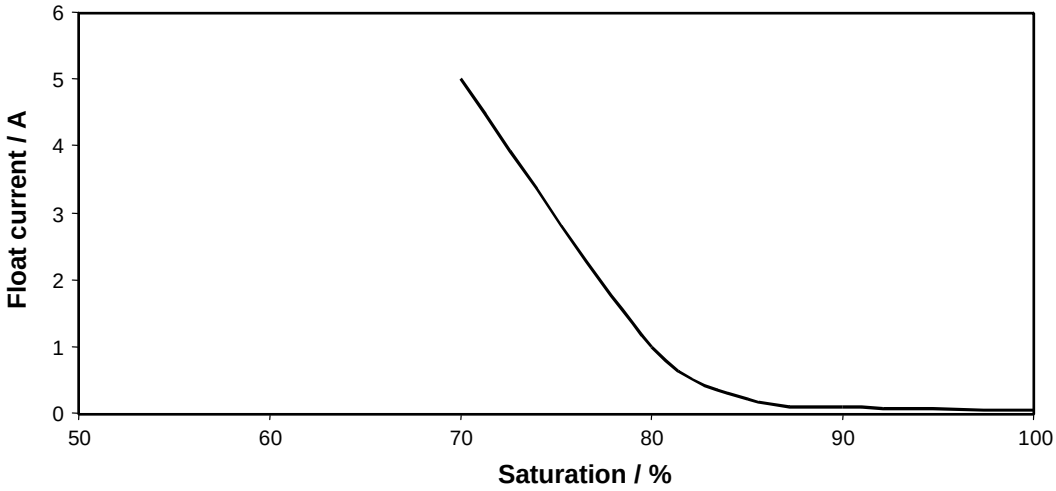

Fig. 6. Effect of separator saturation on float current at 2.28 Vpc.

be higher and so the time period will be shorter but the total A h remain constant. This suggests that thermal runaway occurs at a specific saturation of the separator. This idea was confirmed by a series of experiments in which batteries were filled to different, known levels of saturation and placed on overcharge at 2.28 Vpc. The resultant curve, Fig. 6, shows a stable float current down to a saturation value of around 85%. Beyond this point, the current increases at a rapid and uncontrolled rate, typical of runaway. Consequently, runaway can occur even at these low applied potentials if the saturation is below the critical level. This observation confirms the explanation of runaway given above.

The final section of the current–time curve is the rapid decrease to zero. This can be explained with reference to Fig. 7, which shows the effect of separator saturation on resistance [8]. The resistance in this diagram is given as a ratio of the resistance at 100% saturation. At saturations above 80%, the resistance remains relatively low but below 80% it increases rapidly so, for instance, at 40% saturation it has a resistance 30 times of that in a fully saturated state. It is this rapid rise in separator resistance at low saturation levels that causes the thermal runaway current to fall rapidly.

The effect of separator resistance on all three stages of thermal runaway is worthy of note. At the start of the process, stage 1, the internal resistance of the cell is low, i.e., of the order of 2 mΩ, but as stage 1 progresses and water is lost the internal resistance and subsequent heating effect increases. This accelerates into thermal runaway because of the non-linear relationship between saturation and resistance. When the internal resistance becomes very high, the effect is to reduce the current as the emission of steam regulates the cell temperature to about 90 °C, but the loss of liquid continues to increase resistance exponentially and this results in the termination of the process. Consequently, the relationship between the resistance and saturation of the separator must be considered as part of the complete thermal runaway process.

In summary, the three stages of the thermal runaway curve are as follows:

Stage 1: stable with low recombination and high water loss.
Stage 2: true thermal runaway.

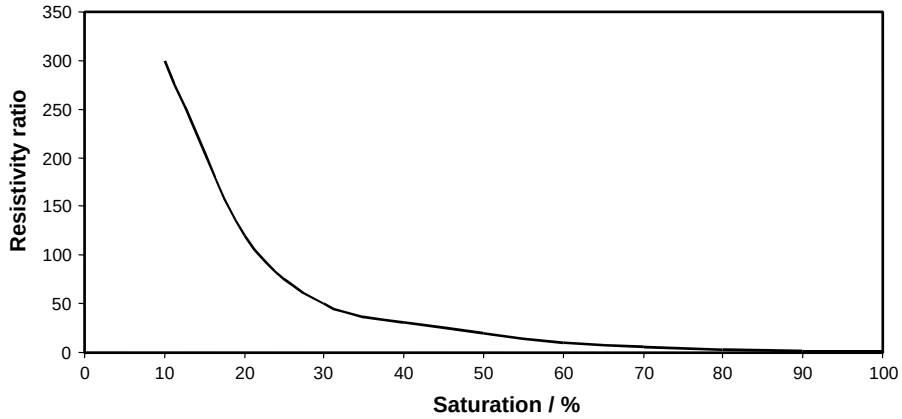

Fig. 7. Effect of separator saturation on resistance.

Stage 3: rapid reduction of the current to zero as a result of the rapid increase in separator resistance.

4.2. Model of separator effect

It has been shown above that thermal runaway occurs when the separator saturation falls below a specific level. This strongly suggests that there is a basic change in a separator property at that critical saturation. Since the main feature of VRLA separators is to allow oxygen transport at high degrees of saturation, it seems likely that it is a change in oxygen transport mechanism that is responsible for the change in behaviour.

It is possible to model the separator by considering it as a regular, three-dimensional, network of cubic-shaped pores with the edges of the pores defined by the rod-like glass fibres. With a single fibre diameter and the fibres distributed at random this gives a 'pore size' of 10 μm, which is of the same order of magnitude of the pores found in actual separators. This is a very simple representation of the separator structure as scanning electron microscopy (SEM) [9] has shown the fibres to be curved rods primarily in the plane of the sheet, while previous work has found the pore structure to be very anisotropic and include a range of pore sizes [8]. Nevertheless, the above simpler model is sufficient to understand the change in oxygen transport mechanism.

For a separator with a thickness of 1 mm, i.e., 100 pores, and initially in a fully saturated state, no oxygen transport in the gas phase will occur. Experience shows that oxygen recombination will begin when the saturation is reduced to 98–95%. If the pores of the model separator are emptied to achieve 98% saturation, the situation becomes as shown in Fig. 8. Here, the pores have been emptied at random as all pores are the same size and there is no preference for which pores will empty first. At these high saturation levels, Fig. 8 shows that there is no continuous open pathway through the separator, so oxygen transport cannot be by pure diffusion but by a pressure-assisted mechanism in which the oxygen pressure forces liquid out of full pores into empty ones to generate a continuous pathway. If the pores are emptied further, at random, eventually the empty pores will line up and create continuous pathways through the separator. This situation is shown in Fig. 9 at a saturation of 80%. It is proposed that it is this change in the open pore structure that is the cause of thermal runaway. At high saturations, oxygen transport is by the pressure-assisted route that gives good recombination efficiencies of the order of 95–97%, but only at low float currents. At low saturations oxygen transport is mainly by pure diffusion and the recombination efficiency is high even at high currents. This large recombination current generates much more heat than when gassing overcharge occurs and thermal runaway results.

Important evidence for this mechanism is given in previous work on the transport of oxygen under zero pressure-gradient conditions, i.e., under diffusion control [8]. This is shown in Fig. 10 where, for the particular separator under test, the oxygen diffusion rate was low and constant between 100 and 90% saturation. The diffusion coefficient measured was that for diffusion of oxygen through a liquid. At a saturation of 90%, the measured diffusion coefficient starts to

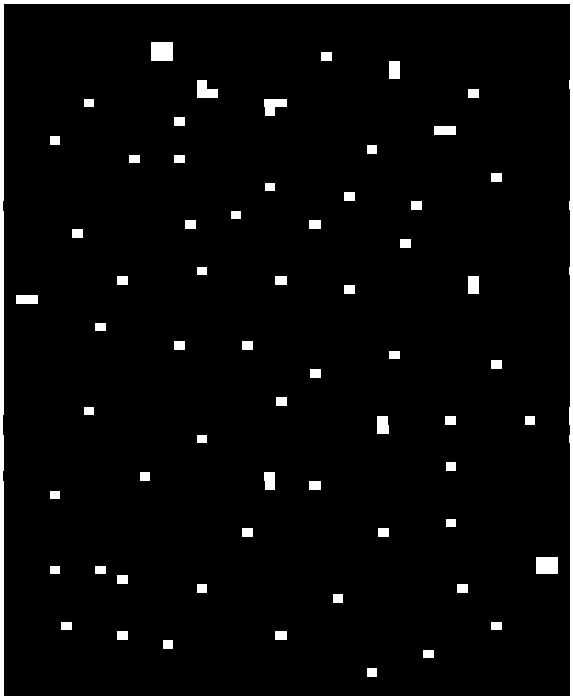

Fig. 8. Model separator at 98% saturation.

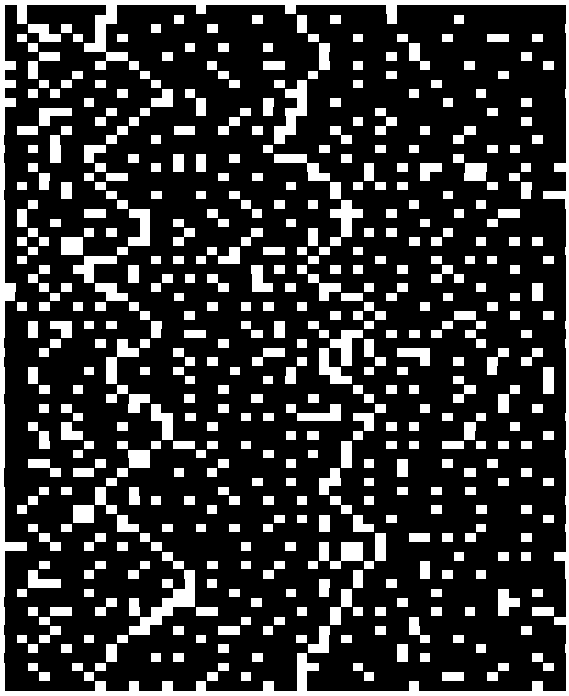

Fig. 9. Model separator at 80% saturation.

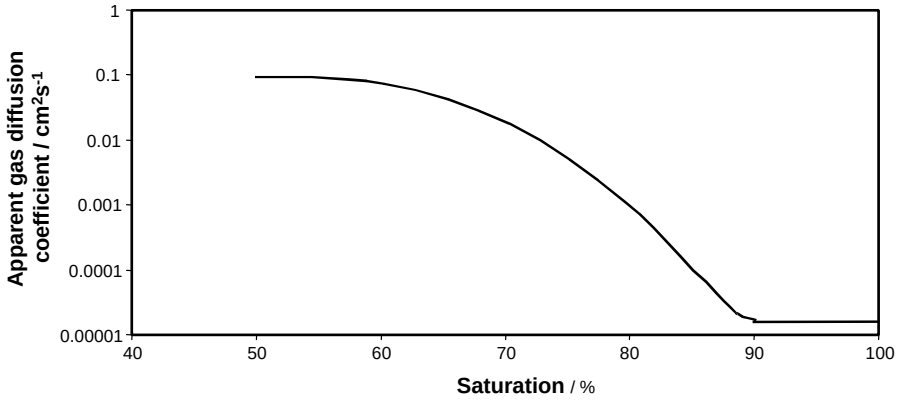

Fig. 10. Effect of separator saturation on oxygen diffusion.

increase rapidly and indicates free diffusion through established gas channels. As the saturation decreases below 90%, more gas channels open up and the effective diffusion coefficient increases.

4.3. Effect of separator structure

The above model considers the pore structure of a separator to be ideal, i.e., all pores have an equal size. This is not true in real separators. Previous work has shown [10] that the pores in the plane of the sheet are smaller than those perpendicular to the plane, and that the pores show a range of diameters. To control the saturation level below which thermal runaway can occur, the pores perpendicular to the sheet must be considered, as these are the ones in which oxygen transport occurs.

The best situation is when all of these pores are of the same diameter so that there is no preference for any pore to empty first and, as the saturation reduces, the pores really do empty at random. For a three-dimensional structure, percolation theory predicts that this transition to continuous open pathways should occur at about 60% saturation. It is interesting to note here that further work on diffusion of oxygen in a different separator has given a transition saturation from liquid to gas phase transport at this level of saturation [11]. As the pore-size distribution increases, there is more chance that pores significantly larger than the mean occur in a continuous pathway to give a large continuous pore through the separator. As capillary pressure determines that these larger pores empty first, it now becomes possible to achieve continuous open gas channels at higher degrees of saturation as shown in this work. Obviously, the greater the pore-size distribution, the higher will be the saturation at which thermal runaway can occur. A good measure for the susceptibility of a separator to thermal runaway would be the difference between the pore size as measured by the maximum bubble pressure technique and the mean pore size. The larger this difference, the higher will be the saturation at which runaway can occur. The maximum bubble pressure technique is particularly valid because it is a direct measure of the capillary pressure of the largest continuous pore perpendicular to the plane of the separator.

4.4. Effect of cell design

To prevent thermal runaway, a VRLA product has to be designed so that the critical saturation level is not reached in service. The properties of the separator obviously impinge on this, as outlined above, but other cell design parameters also have an effect. Anything that affects the rate of water loss, e.g., system purity and rate of grid corrosion, is important. Separator thickness is also important as this acts as an acid reservoir. The thicker the separator, the more acid it will hold and the lower will be the rate of saturation loss for a given rate of water loss. Other parameters such as case thickness, case material and vent efficiency can play minor roles in water loss as can service conditions, frequency of discharging and the method of recharge.

It must be emphasised that at normal float charge voltages of around 2.28 Vpc, the recombination efficiency is so high and the water loss so low that thermal runaway conditions are extremely unlikely to be reached even at the end of life of a battery. This accounts for the very low incidence of reports of batteries failing by thermal runaway.

For batteries seeing frequent deep cycling and recharge at higher voltages without current limit, the situation is not so clear and these may be more susceptible to runaway.

5. Conclusions

Experiments in which 6 V VRLA batteries have been overcharged at potentials of up to 2.65 Vpc and 60 °C show that the applied voltage is the main factor responsible for thermal runaway. Temperature acts only as an accelerating factor.

The runaway process takes place in three distinct stages. In stage 1, recombination efficiency is low, water loss high and temperature and current rise slowly, due to the small and slowly increasing internal resistance and low recombination

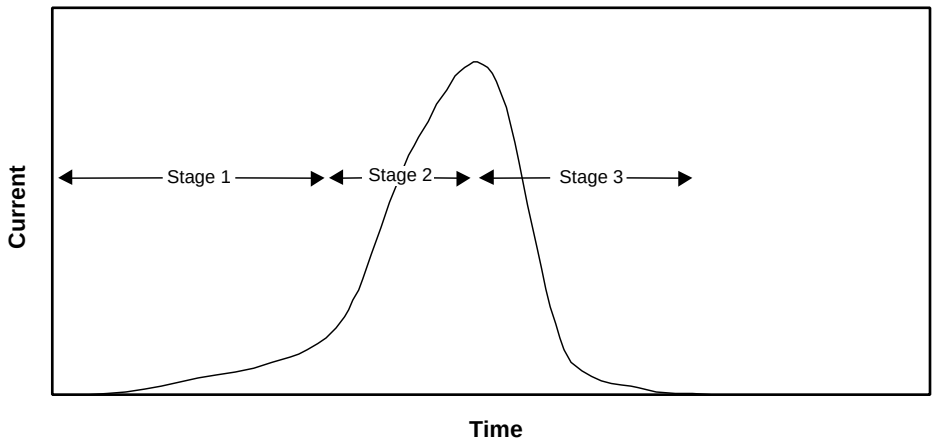

	Stage 1	Stage 2	Stage 3
Current	Stable	Rises rapidly	Falls rapidly
Water Loss	High	Low to high	Low
Recombination	Low	High	High
Internal resistance	Low	High	Very high
RE Mechanism	Pressure assisted	Free diffusion	Free diffusion
Heat generation	Low	High	low

RE = recombination efficiency

Fig. 11. Summary of thermal runaway.

efficiency. In stage 2, the recombination efficiency, even at these high currents is high because of the change in oxygen transport mechanism through the separator. Heat generation increases rapidly because of a combination of increased recombination rate and increased internal resistance of the separator. This process comes to an end when the cell temperature reaches the boiling point of the electrolyte. This controls the temperature but water loss, and hence separator resistance, continues to increase and the current reduces rapidly in stage 3. These changes are summarised in Fig. 11.

The parameter that causes the change from stage 1 to stage 2 is the change in oxygen transport mechanism through the separator. It is postulated that changes in separator design can effect the value of the critical saturation at which this occurs and this, together with cell design parameters and correct in-service conditions, ensures that thermal runaway is not a normal failure mode in service.

References

[1] D.O. Feder, in: Proceedings of the Intelec'95, pp. 22−27.
[2] B. Culpin, D.A.J. Rand, J. Power Sour. 36 (1991) 415–438.
[3] W.T. Rutledge, R.J. Bowers, in: Proceedings of the Intelec'94, pp. 168−171.
[4] D. McMenamin, in: Proceedings of the Intelec'92, pp. 18−21.
[5] D. Berndt, Maintenance Free Batteries, 1st ed., Wiley, New York, 1993, pp. 306−310.
[6] H.D. Thacker, in: Proceedings of the Intelec'92, pp. 47−50.
[7] S. Torigoe, K. Matsumoto, K. Maki, T. Tanako, T. Babaski, in: Proceedings of the Intelec'94, pp. 54−58.
[8] B. Culpin, J. Hayman, in: L.J. Pearce (Ed.), Power Sources 11, Research and Development in Non-mechanical Electrical Power Sources, International Power Sources Symposium Committee, Leatherhead, England, 1986, pp. 45−66.
[9] A.L. Ferreira, in: Proceedings of the Sixth European Lead-acid Battery Conference, Prague, Czechoslovakia, 1998.
[10] B. Culpin, J. Power Sour. 53 (1995) 127–135.
[11] R.J. Ball, R. Evans, R. Stevens, J. Power Sour. 104 (2002) 208–220.